Do not Film

missing pages 7-13

ENGINEERING AND INDUSTRIAL RESEARCH STATION

Quarterly Progress Report #7

NAS8-11334

RESEARCH STUDY FOR DETERMINATION OF LIQUID SURFACE PROFILE IN A CRYOGENIC TANK DURING GAS INJECTION

December 19, 1965 - March 18, 1966

COLLEGE OF ENGINEERING

MISSISSIPPI STATE UNIVERSITY

STATE COLLEGE, MISSISSIPPI

Engineering and Industrial Research Station
College of Engineering
Mississippi State University
P. O. Box 147, State College, Mississippi 39762

Quarterly Progress Report #7, NAS8-11334
RESEARCH STUDY FOR DETERMINATION OF LIQUID SURFACE PROFILE IN A CRYOGENIC TANK DURING GAS INJECTION

Period Covered: December 19, 1965 - March 18, 1966

Authors:

Dr. E. H. Bishop
Dr. W. D. McCain, Jr.
Mr. R. E. Forbes
Mr. W. S. Cagle
Mr. J. T. Smith

Quarterly Progress Report:
Contract Number: NAS8-11334
Control Number: DCN 1-4-50-01218-01 (1F)
CPB 02-1277-64

This report was prepared by Mississippi State University under NAS8-11334 RESEARCH STUDY FOR DETERMINATION OF LIQUID SURFACE PROFILE IN A CRYOGENIC TANK DURING GAS INJECTION, for the George C. Marshall Space Flight Center of the National Aeronautics and Space Administration. The work was administered under the technical direction of the Propulsion and Vehicle Engineering Laboratory, of the George C. Marshall Space Flight Center with Mr. Hugh M. Campbell acting as project manager.

TABLE OF CONTENTS

LIST OF FIGURES

LIST OF FIGURES -- continued

LIST OF TABLES

ABSTRACT

This is the Seventh Quarterly Progress Report for NAS8-11334, DETERMINATION OF LIQUID SURFACE PROFILE IN A CRYOGENIC TANK DURING GAS INJECTION. The period covered is December 19, 1965 - March 18, 1966.

Motion pictures of the surface disturbance caused by swarms of nitrogen bubbles rising in distilled water have been analyzed and surface profiles plotted from data taken from the film. The data for one inlet gas flow rate has been fitted to the fourth degree polynomial

$$Z_c = .295 \left[1 - .050|r| - .086 |r|^2 - .262|r|^2 + .077|r|^4 \right] \qquad (1)$$

with remarkably good agreement.

The data for numerous inlet gas flow rates are in the process of being analyzed.

The rates at which water is entrained by a saturated air stream were experimentally determined for a modified U-tube configuration as a function of air delivery pressure. The test section employed consisted of a horizontal 5-foot length of 4-inch I.D. glass pipe, into which the air was directed vertically downward at one end and from which, at the opposite end, the air and entrained water flowed through a vertical 10-foot length of glass pipe. The water removal rate was determined for various gas delivery pressures and percentage of the horizontal pipe filled with water. Tests were first conducted by gradually increasing the gas delivery pressure until the desired pressure was achieved; then they were repeated by impacting the test section with the same pressures. Curves of the measured entrainment rates for each case studied are presented. Detailed qualitative descriptions and sketches of the flow

phenomona in the horizontal and vertical pipes are given, as well as photographs of the flow at sections of particular interest.

PROGRESS

Surface Profile

The study of the disturbance of the surface of a liquid caused by rising swarms of gas bubbles has begun and is progressing rapidly. The liquid used in the initial work is distilled water. The inlet configuration selected to initiate the swarm of bubbles for the first experimentation may be seen in the photograph in Figure 1. This inlet device consists of nine 26 gauge hypodermic needles arranged in a square pattern. Figures 1 and 2 show that the bubbles formed are reasonably uniform in size. No large, rapidly rising bubbles are formed. Apparently, the bubbles do not coalesce during their rise.

Figure 2 shows three sets of photographic prints taken from the motion picture film. These prints show the disturbance of a liquid surface at three different times selected at random from the film. The prints within each of the three sets are separated in time by five milliseconds. One can observe the approximately constant shape, height, and position of the surface disturbance.

The pictures given in Figure 2 were obtained at the moderately low overall inlet flow rate. At higher flow rates the surface disturbance does not remain stationary but begins to move about, however, the height and shape seem to be fairly constant.

The data on height and shape of these disturbances were obtained in the same manner that we used in the single bubble research. These data are given in Table I and are shown graphically in Figure 3 for an inlet flow rate of 2.01 standard cubic feet per hour of nitrogen gas.

The confidence interval given in Table I is plus or minus about 5%

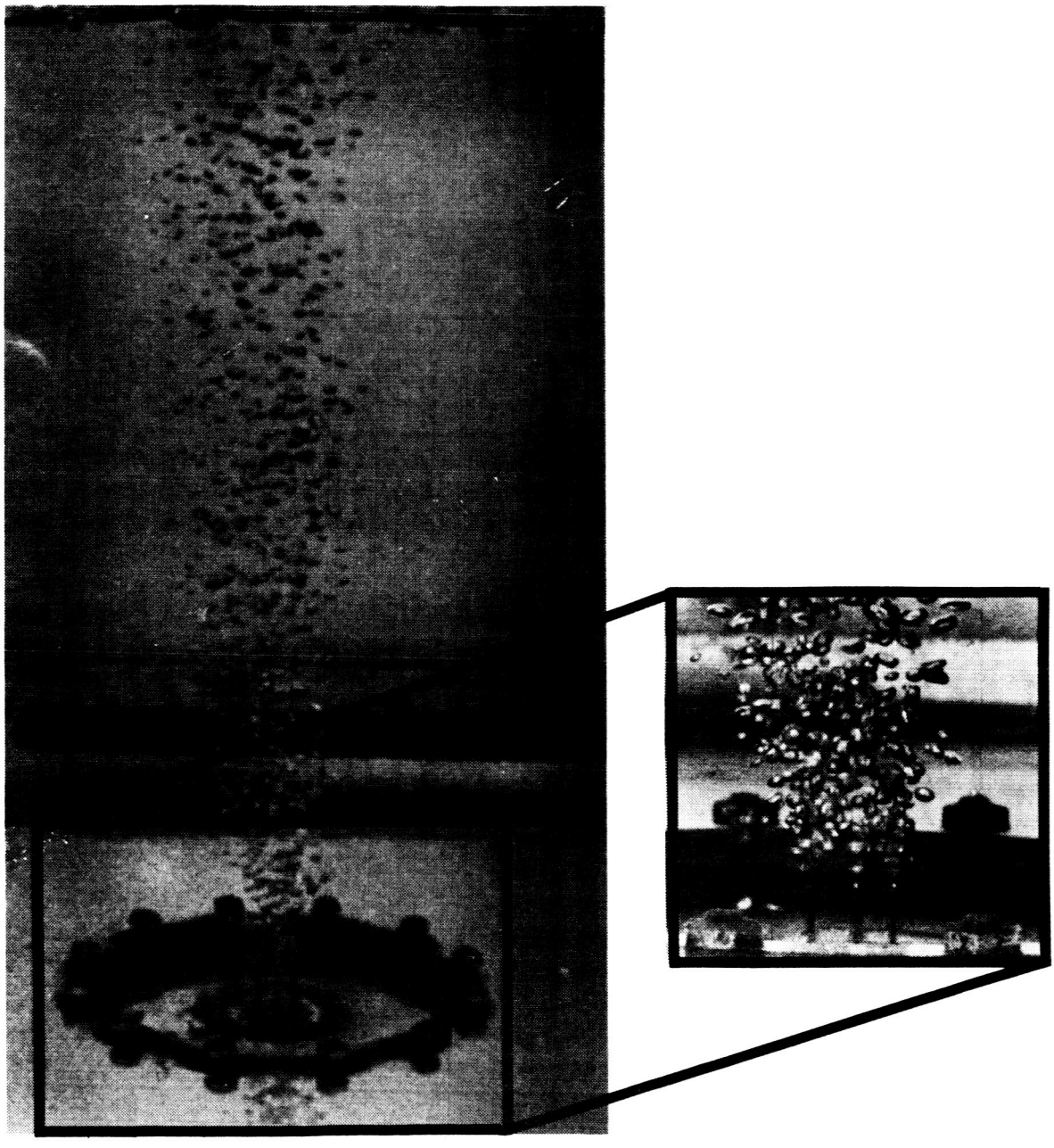

Figure 1. General View of a Typical Swarm of Nitrogen Bubbles Rising in Distilled Water. Inlet Configuration Shown Consists of Nine 26 gauge Hypodermic Needles in a Square Pattern. Surface Disturbance Not Shown.

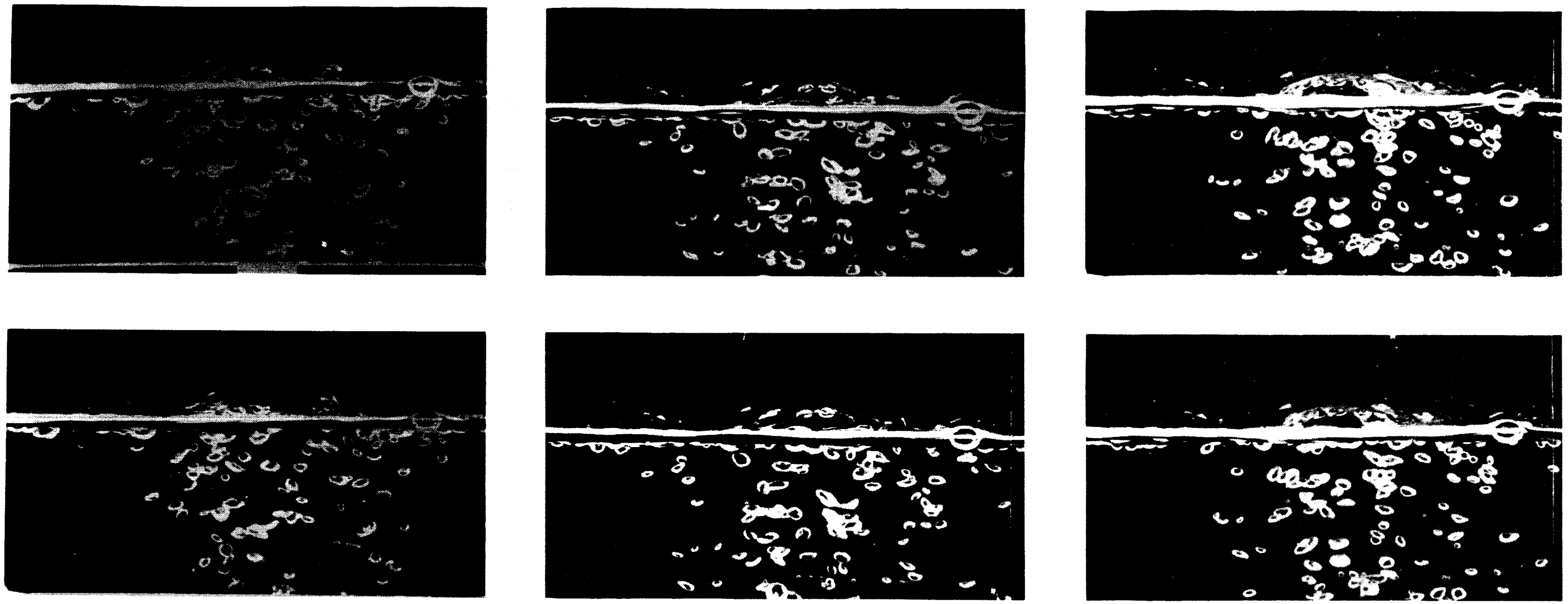

Figure 2. Surface Disturbance Caused by a Swarm of Bubbles of Nitrogen Gas Rising in Distilled Water. Taken from Frames of High Speed, 16 mm, Motion Picture Film. Three Sets of Photographs Taken at Random Times During the Run. The Two Pictures within Each Set are Separated in Time by Five Milliseconds. Overall Inlet Gas Flow Rate of 2.01 Standard Cubic Feet Per Hour.

TABLE I

Experimental Surface Profile Data for a Swarm of Nitrogen Bubbles Rising in Distilled Water at an Overall Gas Flow Rate of 2.01 Standard Cubic Feet/Hr. Through a Square Configuration of Nine 26 Gauge Hypodermic Needles.

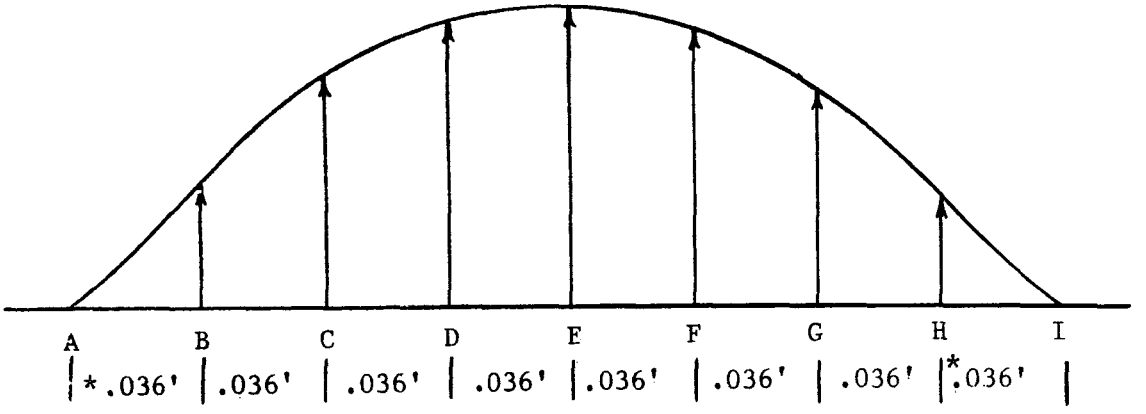

* Average Value

Position (See Diagram Above)	Height of Surface Disturbance above Quiescent Liquid Surface, ft. (Average of 53 Data Points)
A	0.0000 ± 0.0000
B	0.0111 ± 0.0011
C	0.0197 ± 0.0013
D	0.0236 ± 0.0013
E	0.0246 ± 0.0012
F	0.0227 ± 0.0010
G	0.0182 ± 0.0009
H	0.0107 ± 0.0011
I	0.0000 ± 0.0000

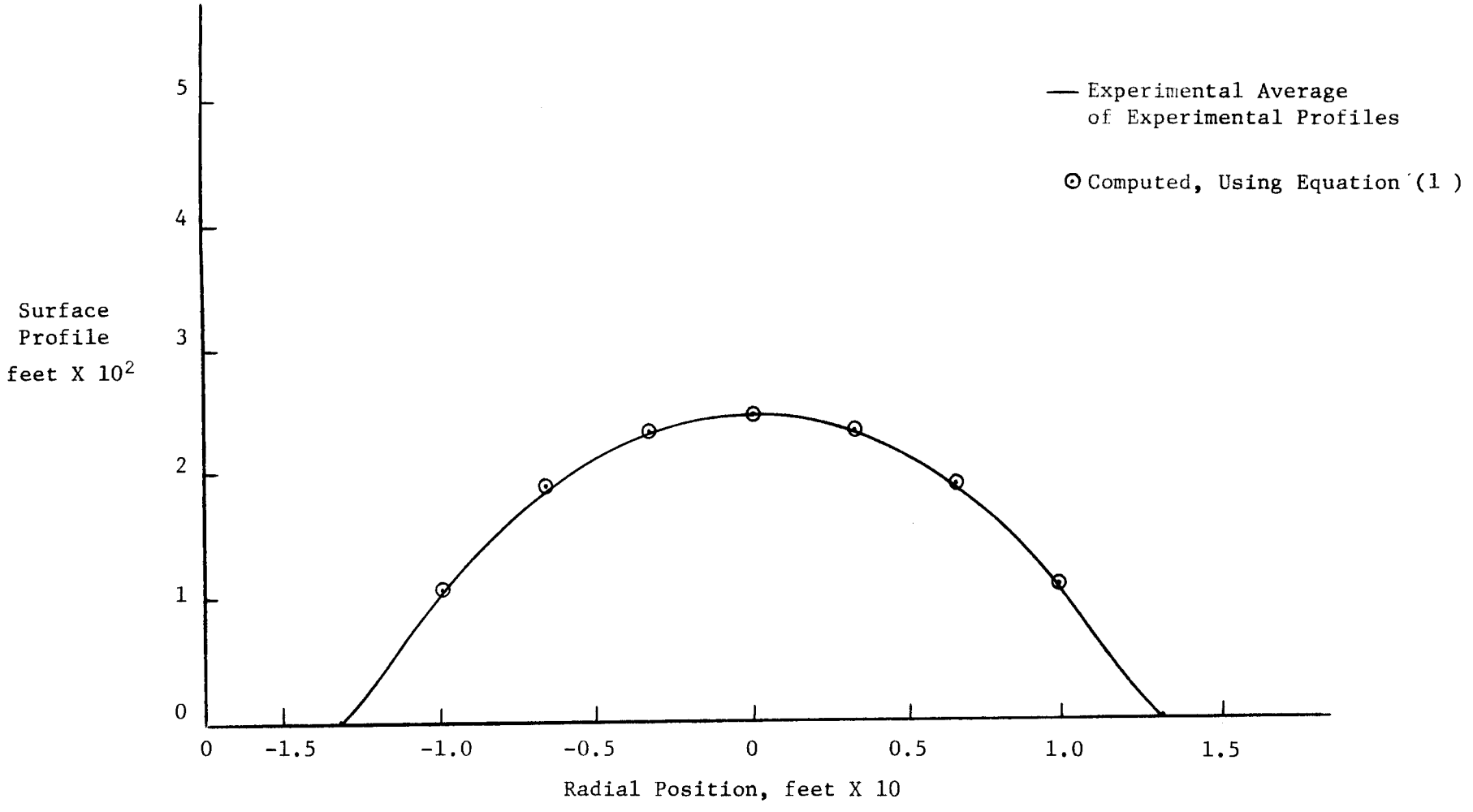

Figure 3. Surface Profile in Distilled Water Caused by a Rising Swarm of Nitrogen Bubbles at an Overall Inlet Gas Flow Rate of 2.01 Standard Cubic Feet Per Hour.

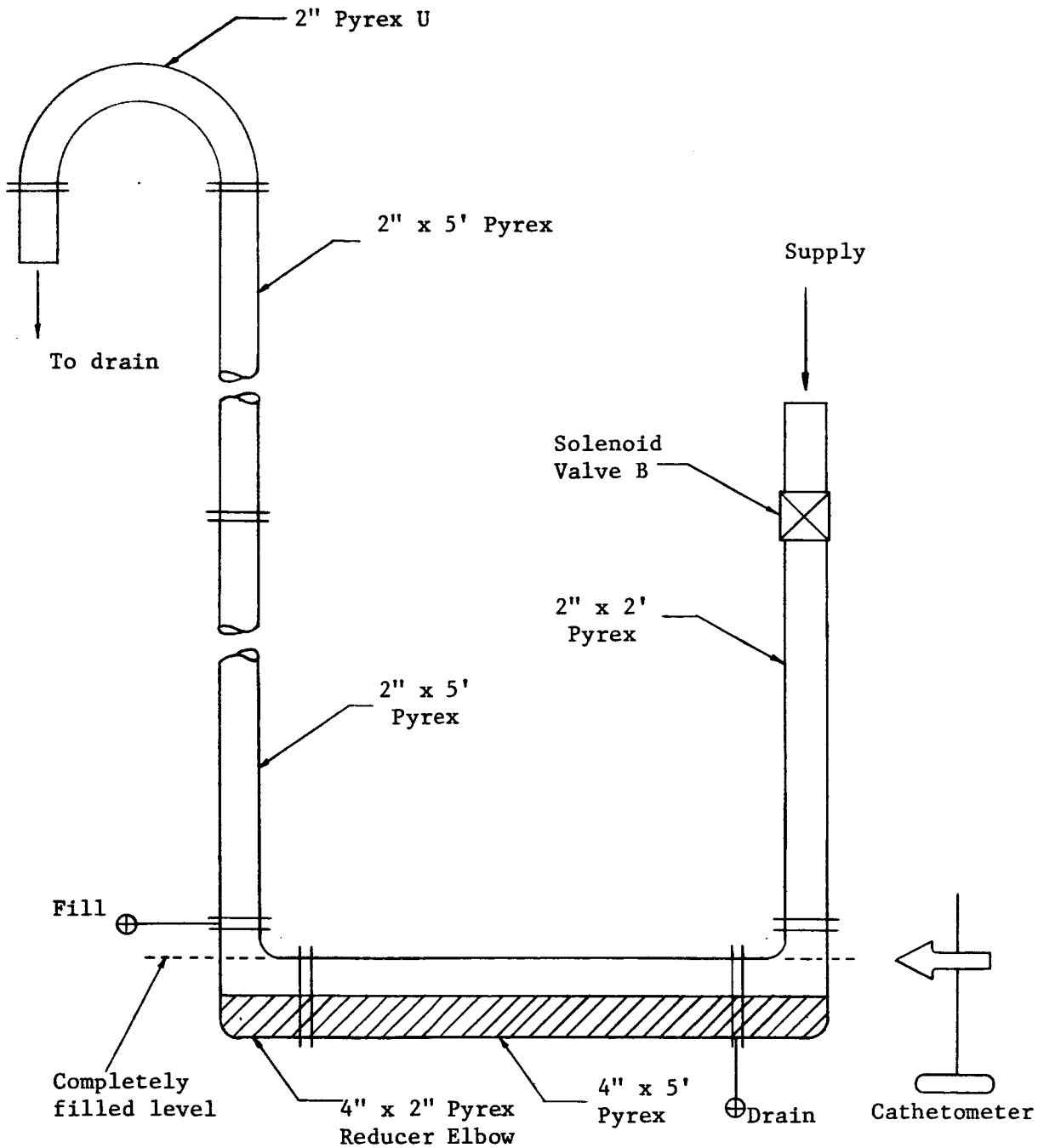

Figure 6. Detailed Drawing of Test Section Shown in Figure 4.

at a value greater than 90 per cent during all runs. The relative humidity was controlled by adjusting a needle valve supplying high pressure steam to the humidifier. The exact procedure for controlling the relative humidity will be discussed in the section on experimental procedures. A specially constructed York Demister was located in the outlet end of the humidifier to remove any water drops entrained in the air stream during the humidifying process. A drain was located in the bottom of the tank to permit the removal of condensed moisture at the end of the day.

The air was carried through two-inch steel pipe from the humidifier to a 42 gallon 125 psi surge tank. The surge tank was used as an added precaution to insure that no surges were imposed on the water in the test section.

Solenoid valves A and B (Figure 4) were connected to the surge tank using two-inch steel pipe. The valve switches were connected so that valve A was open when B was closed and vice versa. The valves were mutually connected using a single-pole double throw switch to insure that the closing of one valve was simultaneous with the opening of the other. When valve A is open and valve B is closed, the air flows through the throttling valve and is exhausted to the atmosphere. The throttling valve is used to adjust the volume flow rate of saturated air through the exhaust section. Dry bulb and wet bulb temperatures were measured immediately ahead of this valve. When valve B is open and valve A is closed, the saturated air is routed to the test section shown in Figure 6.

The test section was constructed of Pyrex-glass pipe to permit visual observation of the entrainment phenomenon. The horizontal section containing the water consisted of a 4-inch by 5-foot section of Pyrex pipe and two 4-inch

by 2-inch Pyrex reducer elbows. Photographs of the test section are shown in Appendix I. The test section was filled and drained through connections provided for this purpose in the pipe flanges. The vertical section following the water filled horizontal section consisted of two 2-inch by 5-foot sections of Pyrex pipe and a 2-inch Pyrex U-bend. A flexible hose was used to carry the air and entrained water to a drain.

Rubber gaskets were initially used at all Pyrex-pipe joints, however, it was found that when the joints were tightened, the gaskets protruded into the pipe and caused flow discontinuities. The use of teflon-asbestos gaskets at all joints reduced this problem to an acceptable level.

Experimental Procedures

The volume of water required to completely fill the test section was determined by filling the test section from a calibrated burette. The test section was considered completely filled when the water reached the level shown in Figure 6. The volume required to completely fill the horizontal pipe was divided into fourths, and tests were conducted at 1/4 and 1/2 of this total amount in order to determine the effect of the water level on the entrainment rates. Entrainment rates for the different configurations (1/4 or 1/2 filled) were determined using the following procedures.

The desired configuration was selected and the desired amount of water was added to the test section. After all waves had settled and the water surface was completely calm, a Welch Scientific Company cathetometer was carefully adjusted until the horizontal hairline was exactly level with the surface of the water. Sightings were taken through the elbow and along the axis of the 4-inch tube (as shown in Figure 6) since optical distortion

was a minimum at this position. Air was then allowed to flow through the test section in order to deposit water on all tube walls. The air flow was stopped and all waves allowed to settle, and an amount of water equal to the amount remaining on the tube walls was then added to the test section by filling until the water surface was again level with the horizontal hairline on the cathetometer. The test section was then ready for an experimental run.

An examination of the air flow variables indicated that the static pressure measured at the flow meter was the only flow variable which could readily be maintained constant throughout a run. The pressure regulator was thus adjusted to the desired static pressure, which was maintained throughout a given run. The minimum pressure used was that pressure which would just initiate water removal in the vertical U-bend. Tests were also run at higher pressures to determine the effect on entrainment rates.

The humidification of the air was accomplished in the following manner. With solenoid valve A open and valve B closed, the pressure regulator was adjusted until the desired pressure was indicated on the manometer. The throttling valve was then adjusted until the volume flow rate through the exhaust section was the same as if the flow were being directed through the test section. This rate was previously determined during the procedure for wetting the walls of the test section. Once the given flow rate was obtained, the steam supply to the humidifier was adjusted until the desired readings were indicated on the wet and dry bulb thermometers.

When the desired relative humidity was obtained, the pressure regulator was momentarily shut off, stopping the air flow, and solenoid valve A was closed and B was opened. The pressure regulator was then opened and the pressure gradually adjusted to the desired level, allowing the saturated air

to go through the test section. The effect of impacting the airstream on the water was studied by using the same general procedures except that the solenoid valves were switched (B opened and A closed) without shutting off the airflow at the pressure regulator.

After the test had been conducted for the desired time, as indicated by a stopwatch, the solenoid valves were switched directing the airflow through the exhaust section. All waves in the test section were allowed to settle and the tube was refilled to the original level using the horizontal hairline on the cathetometer as a reference. The amount of water required to refill the tube was measured using a calibrated burette. This procedure was then repeated at different time intervals to determine the liquid entrainment as a function of time.

Experimental Accuracy

Errors were introduced into the data due to inaccuracy of the volume measurements made using the calibrated burette and the inability to refill the test section to exactly the desired level following a test run.

The burette, with a capacity of 7 liters, was calibrated using a graduated cylinder and a liter flask. Following the calibration, a liter flask could be filled to within plus or minus 5 cubic centimeters of the full level by referring to readings on the burette. The error introduced using the burette is no greater than plus or minus one half of one percent of the water volume required for refilling of the test section.

It was impossible, even with the magnification provided by the cathetometer, to refill the test section to exactly the same level following successive runs. This was due to inconsistencies in the meniscus at the

water glass interface. This error was largest for short runs with a low supply pressure since only small amounts of water were required to refill the test section following such runs. The upper level of this error is estimated at 10 per cent, with a diminishing effect for long runs at high supply pressures.

It was also determined that the cleanliness of the pipe walls had an effect on the entrainment rates. Following several days of tests, a mineral film, resulting from the use of tap water as the test liquid, could be seen on the pipe walls. The walls were cleaned when the test section was disassembled to replace the rubber gaskets, and runs following the pipe cleaning showed that entrainment rates were higher than before the cleaning. At this time no attempt has been made to determine the magnitude of this effect on the entrainment rate. All data were obtained with some trace of mineral deposits on the pipe walls.

Discussion of Results

The rate of removal of an entrapped liquid by a high velocity gas stream depends upon many factors, among which are: geometry of the system, densities and viscosities of the liquid and gas, surface tension of the liquid, gas mass flow rate, gas impingement angle, and the fraction of the volume of the system cross section occupied by the liquid. Because of the large number of variables which are apparently pertinent, the initial experimental results to be discussed in this section should not be considered as applicable to a general system nor to a system of the same geometrical configuration but with different liquids or gases.

The experimental data given in Appendix II were obtained for the

The geometry of this inlet is such that the air strikes the water surface at a right angle as a jet and consequently, if the kinetic energy of the jet is sufficient, removes all water from zone 1 at the initial impact. This is shown in the photograph of Figure 8. The length of this zone is directly dependent on the kinetic energy of the incoming air.

The impact of the air on the water results in the entraining of many droplets into the free air stream. As shown schematically in Figure 7 and in the photograph of Figure 8, the direction of the water droplets is such to cause the droplets to impinge on the top of the horizontal section. Consequently, few, if any, of the droplets entrained in zone 2 traverse the length of the horizontal section without either impinging on the wall of the tube or on the liquid surface of zone 3. Since the incoming air is continually entraining more water than is removed from the horizontal section, there is some backflow into zone 2 as indicated by the arrow at A in Figure 7. Immediately adjacent to this backflow and still in zone 2 is a relatively waveless and motionless area, designated by B, where the waves of zone 3 begin to form. These waves traverse the length of zone 3 with increasing velocity and amplitude and impinge on the end of the horizontal section at D. A photograph of the waves of zone 3 appears in Figure 9. The individual water particle in zone 3 moves in a circular or an ellipsoidal path as the wave passes by. This is a combination of transverse and longitudinal wave motion.

The impingement of the waves at D in Figure 7 and in the photograph of Figure 10 deposits a thin film of water on the surface of the elbow and is the major means by which water is transported from the test section into the vertical tube. The height to which this film will move into the vertical

following system:

(a) Geometrical configuration: see Figure 6

(b) Entrapped liquid: water

(c) Gas stream: saturated air

To insure negligible evaporation of the water into the air, the air was saturated to relative humidities greater than 90%.

Some interesting flow phenomena occur in the horizontal 4-inch section shown in Figure 6. A typical sketch of the flow phenomena is shown below in Figure 7, where, for the purpose of discussion, the horizontal section is divided into three distinct zones, in each of which different flow patterns are evident. Zone 1 extends for the first few inches of the horizontal test section and generally contains no water. (For low air flow rates, water remains in this zone.)

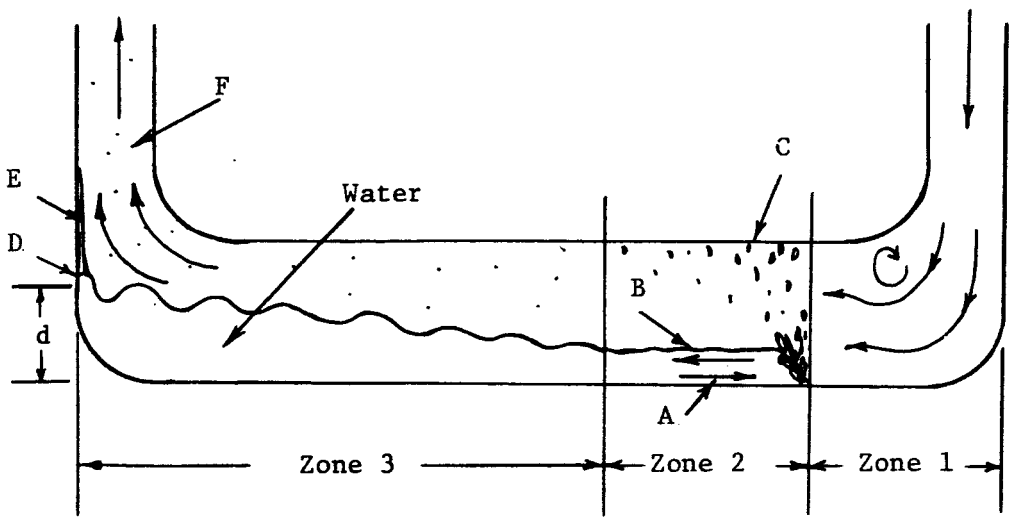

Figure 7. Flow Phenomena in Horizontal Section.

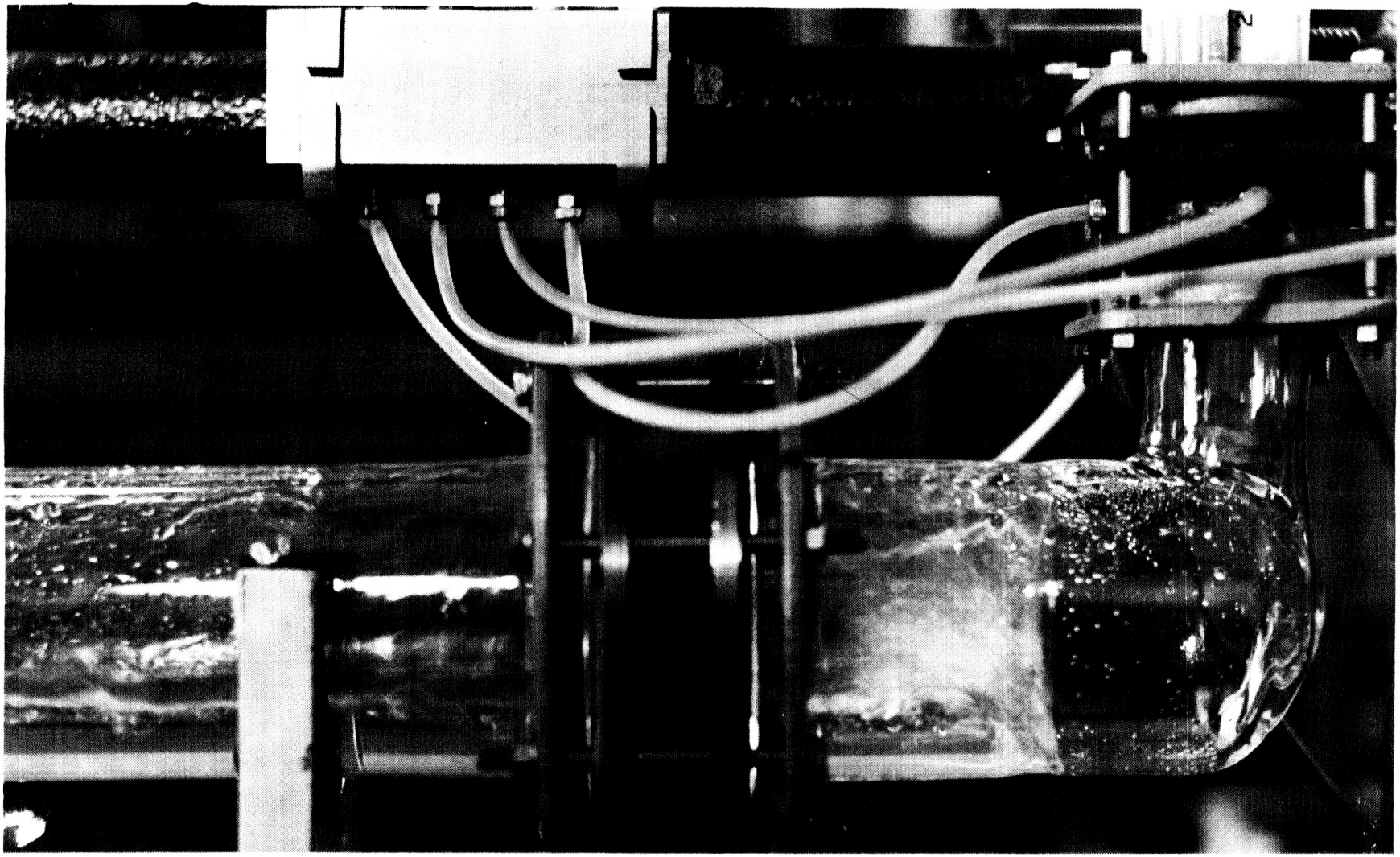

Figure 8. Photograph of zones 1 and 2 showing absence of water in Zone 1 and the water spray and droplets impinging on the surface of the horizontal pipe.

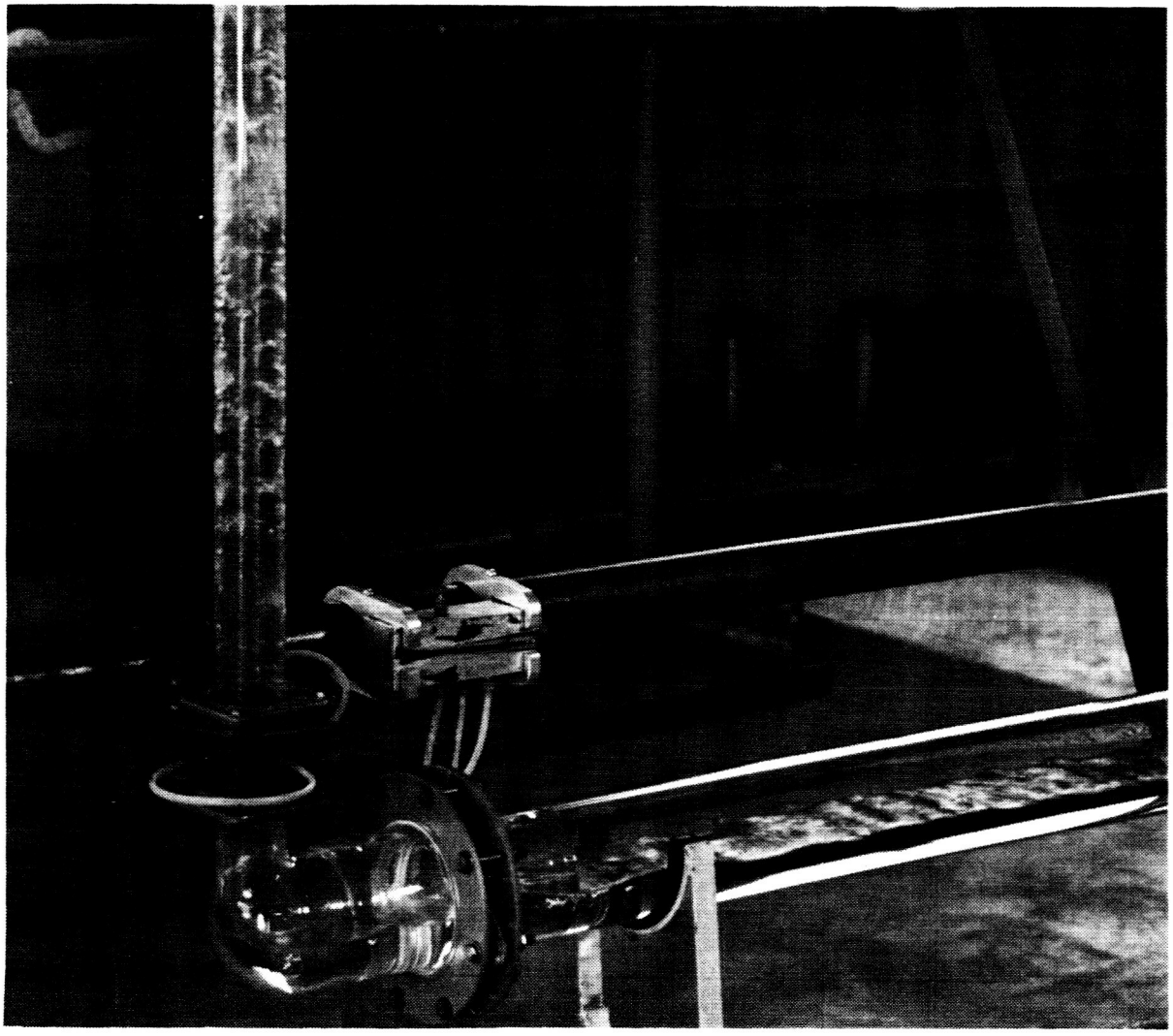

Figure 9. Photograph of zone 3 showing waves in horizontal pipe and the oscillating turbulent film in the vertical pipe.

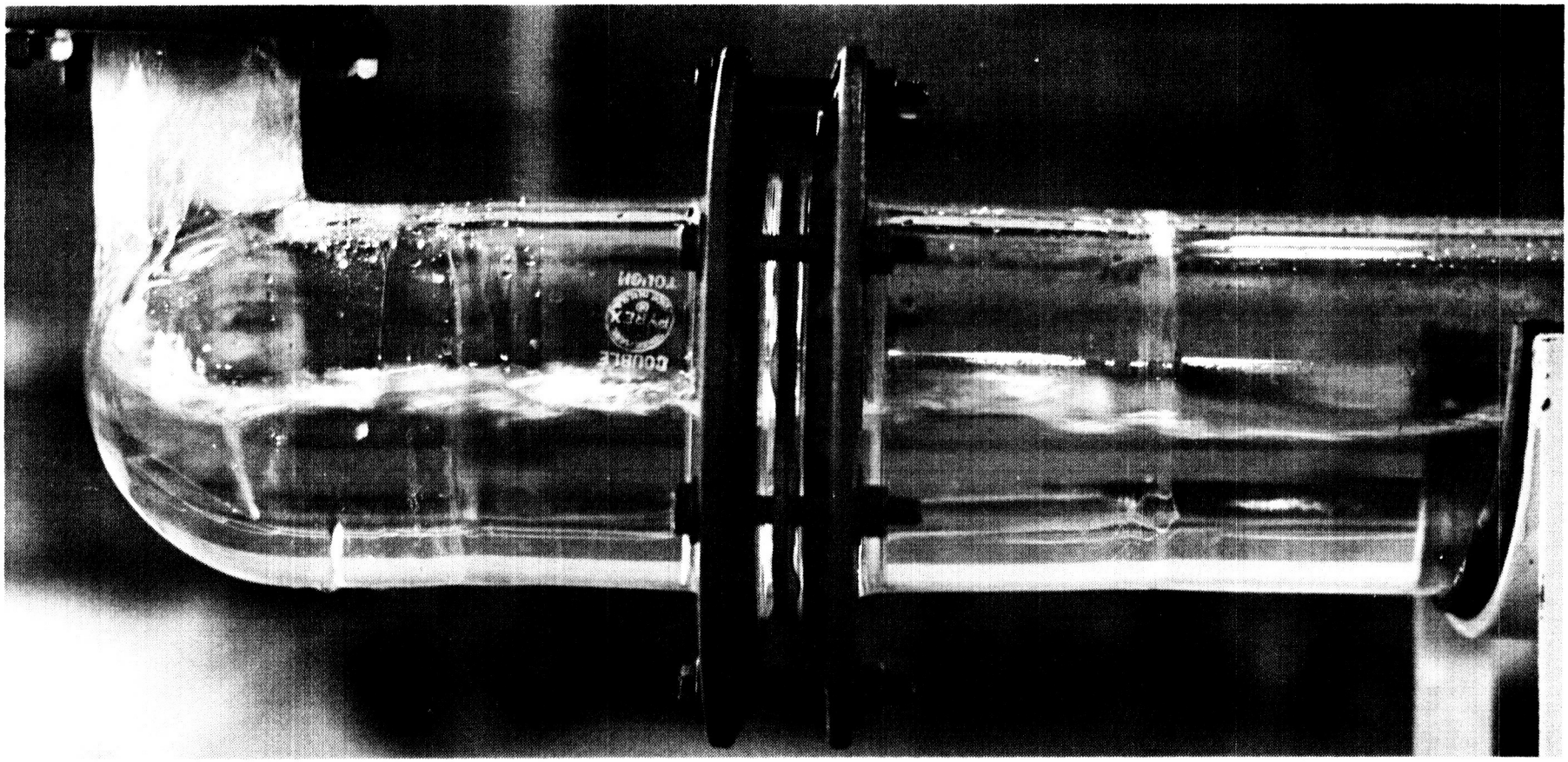

Figure 10. Photograph of the waves impinging on the elbow at D of Figure 7.

section F of Figure 7 is directly dependent on the velocity of the air, since the film is moved upward by the viscous drag exerted by the flowing air. As water is carried out of the vertical pipe, the film is replenished by the impingement of each successive wave on the elbow at D.

The height to which a wave splashes when it impinges on the elbow at D of Figure 7 and, as a result, the amount of water which reaches the vertical pipe F, depends on its amplitude, velocity, and the average depth $\underline{d}$ of the water at D. Since the wave velocity and amplitude depend on the distance the wave travels, the amount of water which feeds the film at E is a function of the length of the horizontal section. The influence of the average depth $\underline{d}$ of the water at D is to control the maximum height to which a wave with a given velocity and amplitude splashes. Consequently, for a given air flow rate, the amount of water removed from the test section via the flowing film will increase as the average depth $\underline{d}$ increases.

Just as in the horizontal 4-inch section, varied flow phenomena may be observed in the 2-inch vertical pipe as shown schematically in Figure 11 and in the photograph of Figure 9 and Figure 12. The various flow phenomena here are attributed primarily to the air velocity. For mass flow rates less than 5.53 lbm per min., the flow phenomena shown in (a) of Figure 11 and in the photograph of Figure 9 occur; whereas, for mass flow rates greater than 5.53 lbm per min., the phenomena shown in (b) of Figure 11 and in the photograph of Figure 12 occur. In both (a) and (b), the annular film is fed by the water deposited at E in Figure 7 when the waves traveling along the horizontal section strike the elbow at D. In Figure 11, the flow in (a) may be termed annular-mist and that of (b) annular. The mist in (a) consists of those droplets produced in zone 2 of Figure 7 which reach the vertical section

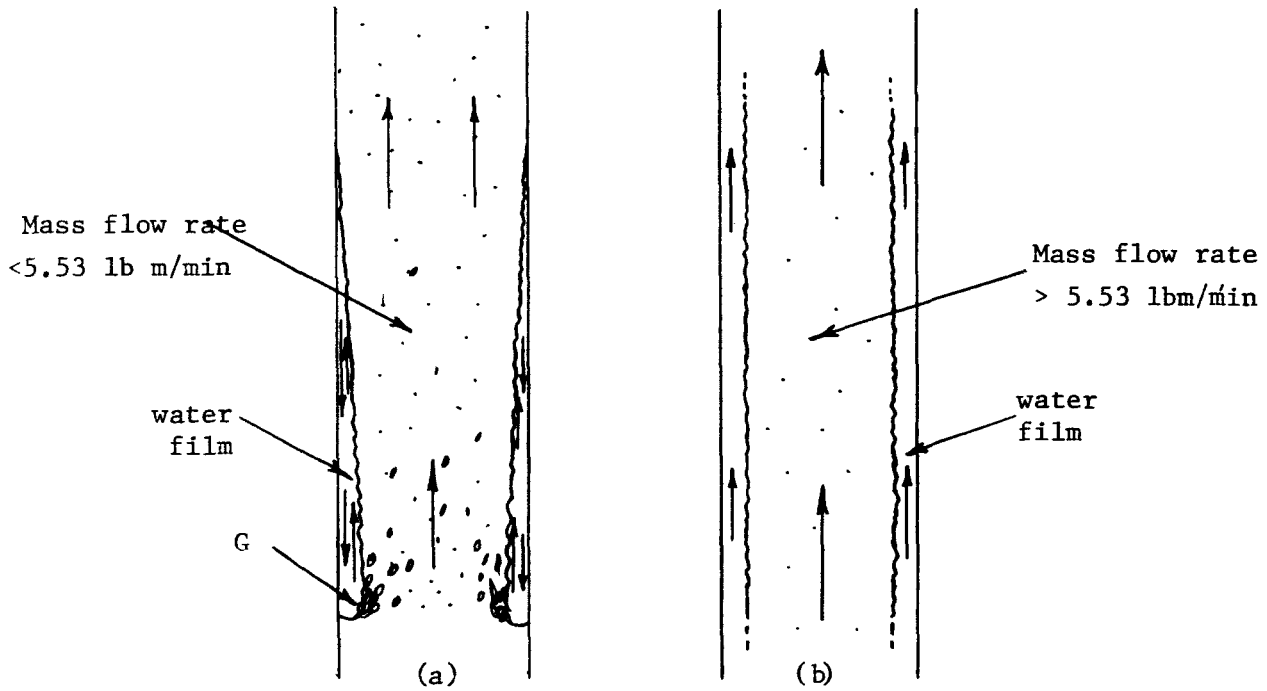

Figure 11. Flow Phenomena in Vertical 2-Inch Pipe.

and those which are entrained by the air stream at G when the fluid flowing adjacent to the vertical tube wall attempts to flow down into the horizontal section. At this point, the fluid is continuously atomized into fine droplets which travel up the vertical pipe a distance which depends on the droplet size and the air velocity. Those droplets which have enough energy imparted to them by the flowing air remain entrained and are subsequently removed from the test system. Those droplets which impinge on the vertical wall or which do not have enough kinetic energy imparted to them by the flowing air collect and fall back down the tubing wall and continuously feed the oscillating, turbulent film on the vertical tubing wall.

In (b) of Figure 11, the air velocity is great enough to impart sufficient kinetic energy to the annular film to transport the film continually up the vertical tube until the fluid reaches the exit and is thus

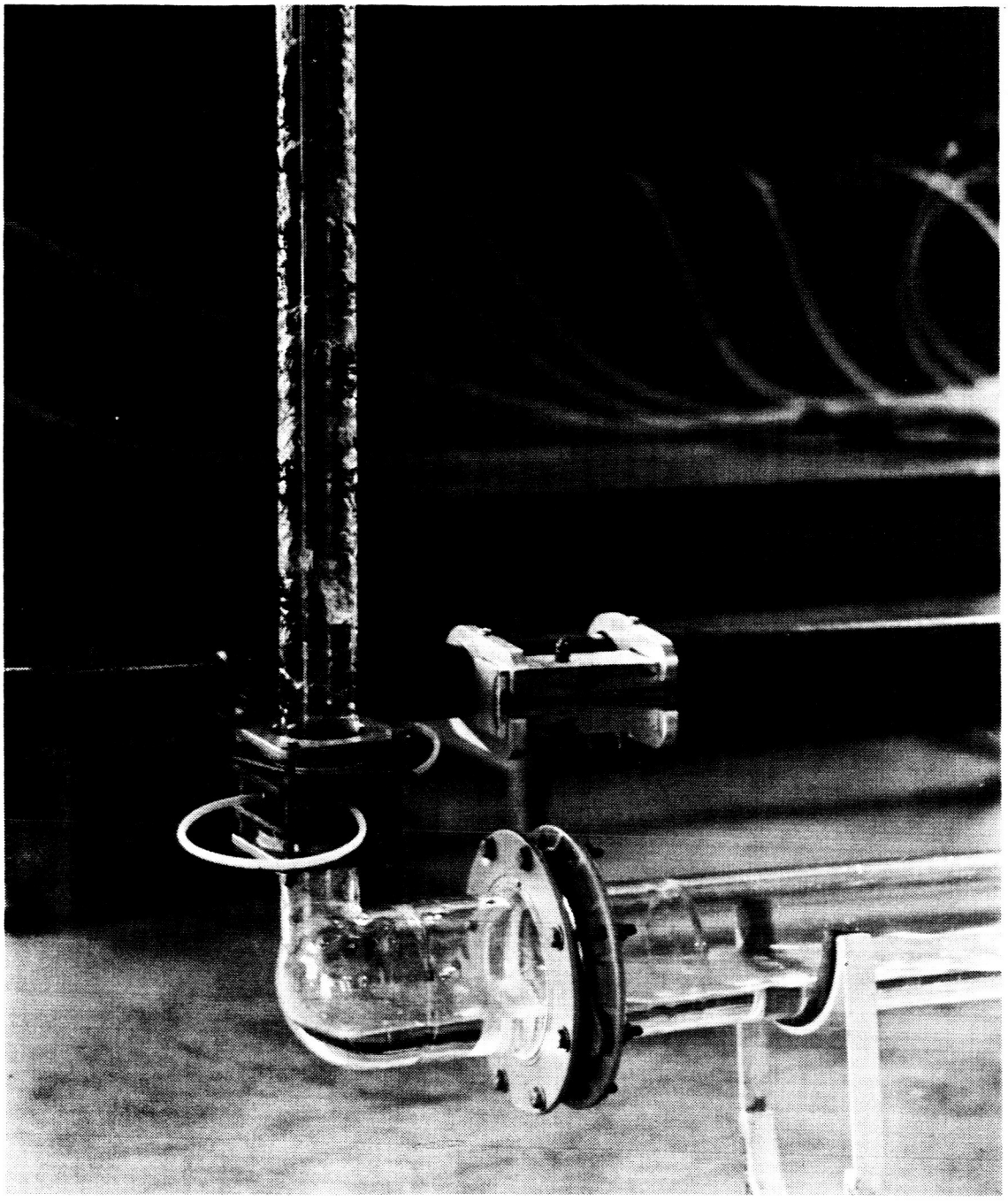

Figure 12. Photograph showing the film in the vertical pipe corresponding to the type sketched in Figure 11(b).

removed from the system. Since the fluid at no time flows down the wall of the tubing, as in (a) of Figure 11, a negligible amount of mist is present.

The rate of removal of fluid from the test section varies with time and never does reach a condition of steady state. As fluid is removed continually, the cross-sectional area available for air flow increases, resulting in a smaller pressure drop across the test section. Consequently, the pressure regulator in Figure 4 opens to supply more air to hold the upstream static pressure constant. (This results in a decrease in the air velocity through the test section. This decrease in velocity is one of the controlling factors in the decrease of removal rate.)

Water entrainment rates are shown in Figures 13 and 14 as amount of water removed divided by amount of water originally entrapped. The solid curves represent removal for a gradual increase in pressure from zero to the static pressure shown as a parameter on the individual curves. The dotted curves represent the fraction removed by impacting the water instantaneously with the air flowing at the same mass flow rate and pressure as for the curve which represents the fraction removed for the gradual increase in pressure.

Note in Figures 13 and 14 that for the lower pressures, impacting the water removes more water initially than does the gradual increase in pressure; however, the total fractions removed are equal as evidenced by the merging of the curves. When the kinetic energy imparted to the stationary water by the impact of the air becomes great enough, more water is removed by the initial impact than during the whole run for a gradual increase in pressure. This is evidenced by the curves for which the pressure is 5.6 inches of mercury in Figure 14.

In Figures 13 and 14 the bottom solid curve represents the minimum

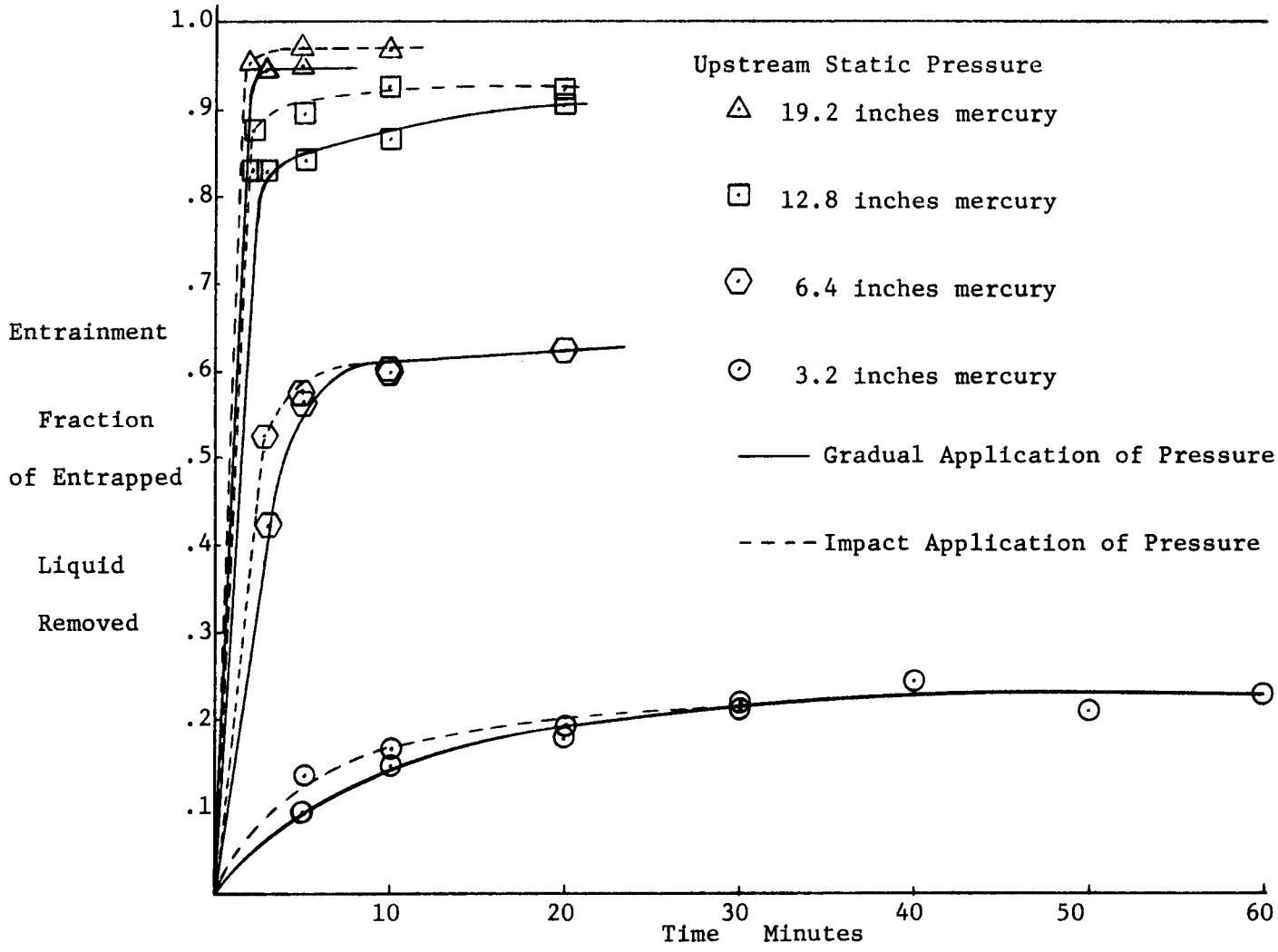

Figure 13. Water entrainment versus time for configuration shown in Figure 6 (1/4 filled) for various upstream static pressures applied both as a gradual increase in pressure and as a sudden impact.

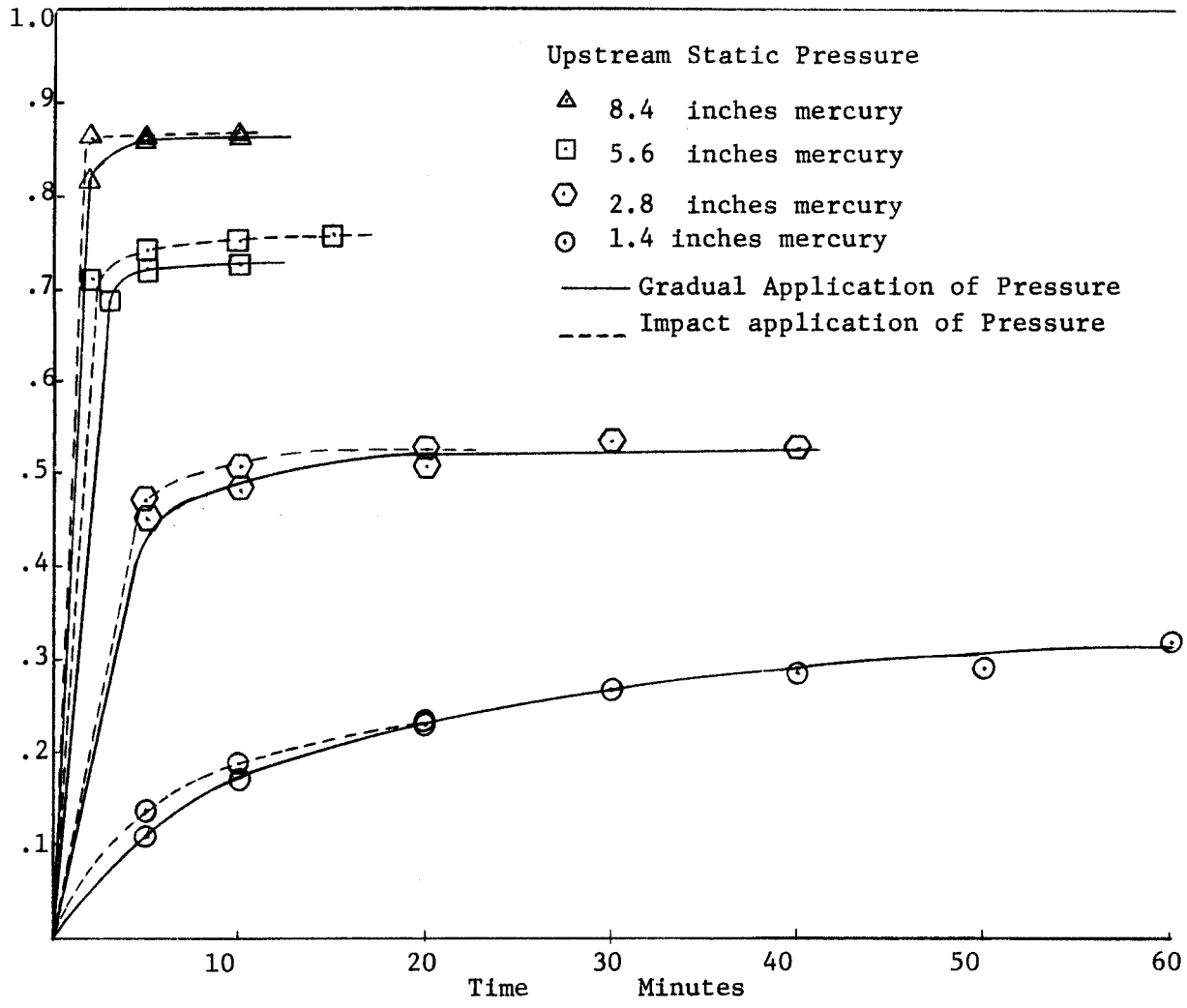

Figure 14. Water entrainment versus time for configuration shown in Figure 6 (1/2 filled) for various upstream static pressures applied both as a gradual increase in pressure and as a sudden impact.

static pressure and average mass flow rate for which a measurable amount of fluid was removed from the test section. Note in Figure 13, that for the 1/4 filled test section, a static pressure of 3.2 inches of mercury was required to initiate withdrawal; whereas, for the half filled test section a substantially lower static pressure of 1.4 inches of mercury was required. The reason for this can be explained in light of what has previously been said about the effect of changing the average depth d of the water at D in Figure 7. For a given air velocity, the maximum height reach by the waves as they impinge at D will be considerably higher for the half filled test section than for the quarter-filled test section.

Reference to Figures 13 and 14 indicate that, except for the minimum pressure to initiate removal, at least ninety per cent of the water was removed from the system in the first five minutes of the run. This indicates that little is accomplished toward the removal of the water from the system after the first five minutes of the run.

CURRENT PROBLEMS

Surface Profile

There are no problems delaying work on the surface disturbance phase of this research and the work is progressing rapidly.

Entrainment

Considerable difficulty was initially encountered in obtaining reproducible entrainment data. These difficulties were caused by experimental inaccuracies in the measurement of the amount of water removed after a given time period. The original method of making these measurements was changed, and by using a cathetometer to establish an initial liquid level accurately, sufficient reproducibility was obtained. However, several weeks of experimental tests had to be repeated. At the present time, the entrainment study is proceeding without any serious problems.

PLANS FOR NEXT QUARTER

Surface Profile

The experimental work on the surface disturbances for distilled water will be completed early in the next quarter. Experimental observations will begin using isopentane as the liquid.

Correlation work concerning the effect of overall inlet gas flow rate on disturbance height should be put into good order prior to the end of the next quarter. This correlation work will be based on the theoretical results given in the Annual Report (2).

Entrainment

The experimental phase of the entrainment study will continue with tests to be conducted on the following geometrical configurations: (Note: test section numbers refer to the geometrical configurations described in Quarterly Progress Report #5)

a) Test Section 3 - 2" I.D. horizontal pipe

b) Test Section 4

c) Test Section 5

The same general experimental procedure followed during this past quarter will be used to conduct the initial tests on the above test sections, and the results will also be presented in a similar manner. Initial attempts will be made to obtain some type of cross-correlation for prediction of the entrainment rate for the various test sections studied utilizing appropriate nondimensional parameters.

APPENDIX I

Photographs of Entrainment Apparatus

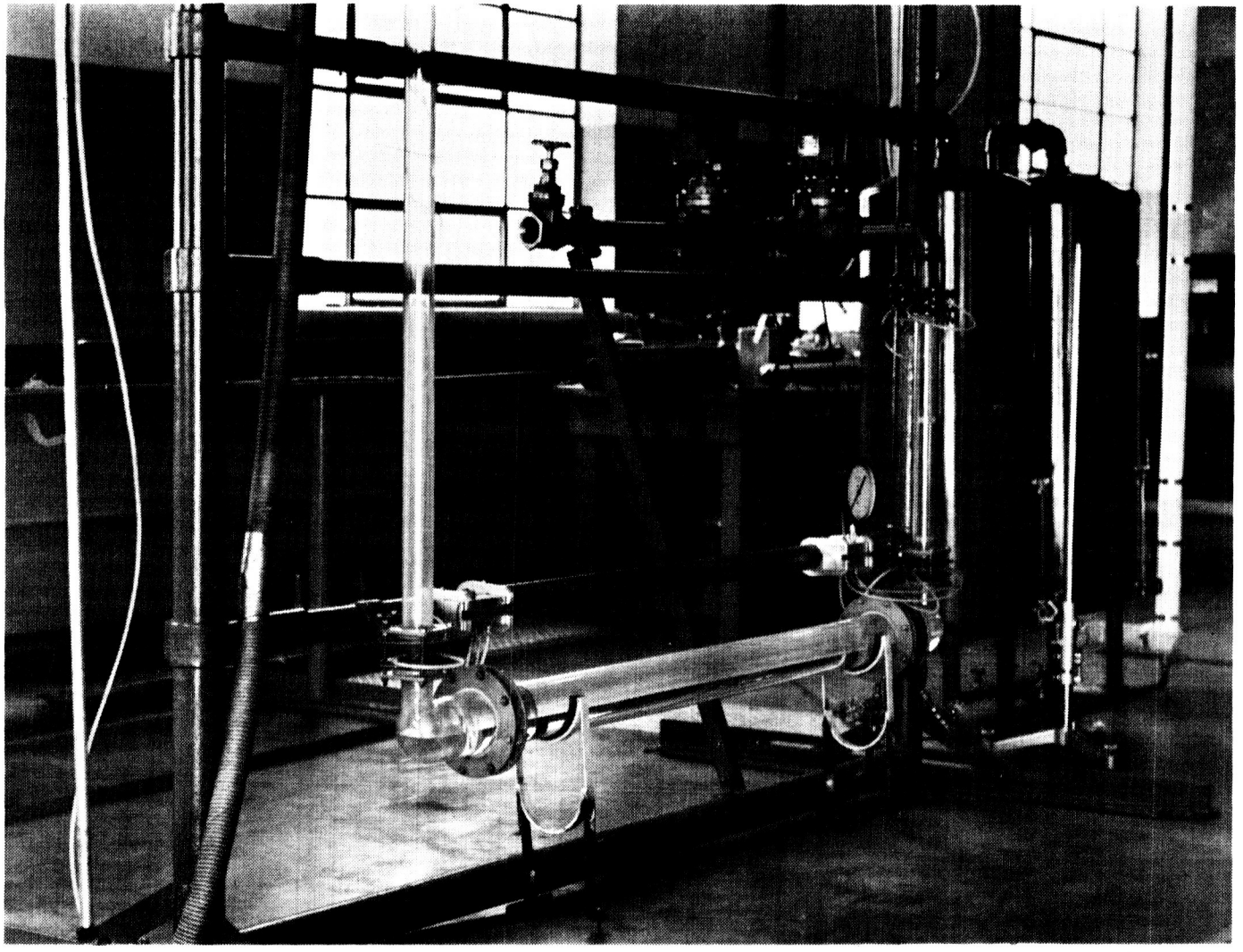

Figure 15. Photograph of overall experimental system.

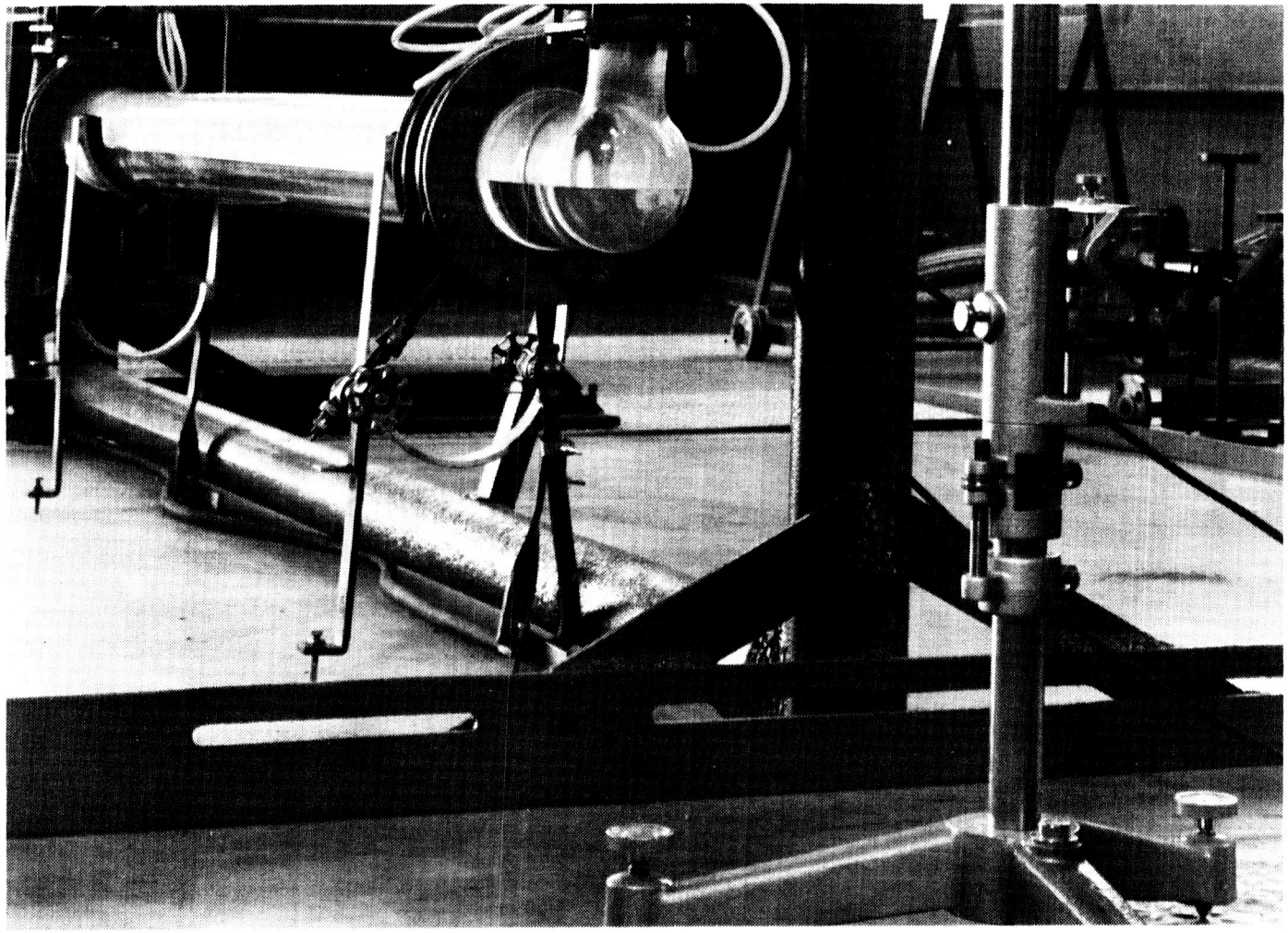

Figure 16. Photograph showing cathetometer position for establishing the initial liquid level.

APPENDIX II

Tabulated Entrainment Data

Time Minutes	Upstream Static Pressure Inches Mercury	Average Mass Flow Rate of Dry Air Pounds Mass Per Minute	Entrainment Fraction of Entrapped Liquid Removed
0 5	3.2	6.877	.09
0 10	3.2	6.853	.15
0 20	3.2	6.889	.18
0 30	3.2	6.968	.22
0 40	3.2	6.888	.25
0 50	3.2	6.714	.21
0 60	3.2	6.698	.22
0 3	6.4	9.409	.42
0 5	6.4	9.437	.57
0 10	6.4	9.629	.60
0 20	6.4	9.339	.63
0 2	12.8	14.056	.83
0 3	12.8	13.875	.83
0 5	12.8	13.990	.84
0 10	12.8	14.219	.87
0 20	12.8	14.308	.90
0 3	19.2	19.261	.94
0 5	19.2	19.324	.94

Table II. Water entrainment versus time for configuration shown in Figure 6 (1/4 filled) for various upstream static pressures applied as a gradual increase.

Time Minutes	Upstream Static Pressure Inches Mercury	Average Mass Flow Rate of Dry Air Pounds Mass Per Minute	Entrainment Fraction of Entrapped Liquid Removed
0 5 0	3.2	6.810	.14
10 0	3.2	6.809	.16
20 0	3.2	6.750	.19
30	3.2	6.760	.21
0 3 0	6.4	9.609	.53
5 0	6.4	9.576	.57
10	6.4	9.611	.60
0 2 0	12.8	14.344	.88
5 0	12.8	14.263	.90
10 0	12.8	14.257	.93
20	12.8	14.184	.92
0 2 0	19.2	19.612	.95
5 0	19.2	19.368	.97
10	19.2	19.381	.97

Table III. Water entrainment versus time for configuration shown in Figure 6 (1/4 filled) for various upstream static pressures applied as a sudden impact.

Time Minutes	Upstream Static Pressure Inches Mercury	Average Mass Flow Rate of Dry Air Pounds Mass Per Minute	Entrainment Fraction of Entrapped Liquid Removed
0 5	1.4	3.445	.11
0 10	1.4	3.422	.17
0 20	1.4	3.652	.23
0 30	1.4	3.770	.27
0 40	1.4	3.643	.29
0 50	1.4	3.667	.29
0 60	1.4	3.655	.32
0 5	2.8	5.529	.46
0 10	2.8	5.615	.48
0 20	2.8	5.414	.51
0 30	2.8	5.737	.54
0 40	2.8	5.722	.53
0 3	5.6	8.595	.69
0 5	5.6	8.418	.72
0 10	5.6	8.317	.73
0 2	8.4	10.771	.82
0 5	8.4	10.666	.86
0 10	8.4	10.786	.86

Table IV. Water entrainment versus time for configuration shown in Figure 6 (1/2 filled) for various upstream static pressures applied as a gradual increase.

Time Minutes	Upstream Static Pressure Inches Mercury	Average Mass Flow Rate of Dry Air Pounds Mass Per Minute	Entrainment Fraction of Entrapped Liquid Removed
0 5	1.4	3.621	.14
0 10	1.4	3.500	.19
0 20	1.4	3.425	.23
0 5	2.8	5.688	.47
0 10	2.8	5.659	.50
0 20	2.8	5.588	.53
0 2	5.6	8.370	.71
0 5	5.6	8.404	.75
0 10	5.6	8.379	.76
0 15	5.6	8.424	.77
0 2	8.4	10.832	.86
0 5	8.4	11.025	.86
0 10	8.4	11.025	.86

Table V. Water entrainment versus time for configuration shown in Figure 6 (1/2 filled) for various upstream static pressures applied as a sudden impact.

BIBLIOGRAPHY

1. Bishop, E. H. and McCain, W. D., Jr., Research Study for the Determination of Liquid Surface Profile in a Cryogenic Tank During Gas Injection, Annual Report, NAS8-11334, Engineering and Industrial Research Station, Mississippi State University, State College, Mississippi, June 17, 1965, p. 24

2. Bishop, E. H., and McCain, W. D., Jr., Research Study for the Determination of Liquid Surface Profile in a Cryogenic Tank During Gas Injection, Annual Report, NAS8-11334, Engineering and Industrial Research Station, Mississippi State University, State College, Mississippi, June 17, 1965, p. 25.